

# MODIS ATMOSPHERIC PROFILE RETRIEVAL ALGORITHM THEORETICAL BASIS DOCUMENT

W. PAUL MENZEL<sup>1</sup>, SUZANNE W. SEEMANN<sup>2</sup>, JUN LI<sup>2</sup>, LIAM E. GUMLEY<sup>2</sup>

*University of Wisconsin-Madison*

*1225 W. Dayton St.*

*Madison, WI 53706*

Version 5

June 7, 2002

---

<sup>1</sup> NOAA/NESDIS (Paul.Menzel@ssec.wisc.edu)

<sup>2</sup> Cooperative Institute for Meteorological Satellite Studies (Suzanne.Seemann@ssec.wisc.edu)

## TABLE OF CONTENTS

1. Introduction .....	1
2. Overview and background information .....	1
2.1 Objectives .....	2
2.2 History .....	2
2.3 Instrument Characteristics .....	3
3. Algorithm Description .....	6
3.1 Theoretical Background .....	6
3.2 Statistical Regression Profile Retrieval .....	7
3.3 Physical Profile Retrieval .....	10
3.4 Derived Products .....	11
3.4.1 Total Column Precipitable Water Vapor and Ozone .....	11
3.4.2 Atmospheric Stability .....	12
4. Operational Retrieval Implementation .....	13
4.1 Cloud Detection Algorithm .....	13
4.2 Radiance Bias Adjustment .....	13
4.3 Adjustments to the NOAA-88b Training Data Set .....	15
4.4 Surface emissivity for IR 4.5 $\mu\text{m}$ spectral bands .....	15
5. Validation of MODIS MOD07 products .....	17
5.1 Comparison of MODIS temperature and moisture with ARM-CART observations.....	17
5.2 Continental-scale comparisons between MODIS and GOES TPW .....	19
5.3 Global comparisons of MODIS products with SSM/I and TOMS .....	21
6. Technical Issues.....	24
7. Future Work .....	27
8. References .....	31

## 1. *Introduction*

The purpose of this document is to present an algorithm for retrieving vertical profiles of atmospheric temperature and moisture from multi-wavelength thermal radiation measurements in clear skies. While the MODIS is not a sounding instrument, it does have many of the spectral bands found on the High resolution Infrared Radiation Sounder (HIRS) currently in service on the polar orbiting NOAA TIROS Operational Vertical Sounder (TOVS). Thus it is possible to generate profiles of temperature and moisture as well as total column estimates of precipitable water vapor, ozone, and atmospheric stability from the MODIS infrared radiance measurements. These parameters can be used to correct for atmospheric effects for some of the MODIS products (such as sea surface and land surface temperatures, ocean aerosol properties, water leaving radiances, photosynthetically active radiation) as well as to characterize the atmospheric state for global greenhouse studies. The MODIS algorithms were adapted from the operational HIRS and GOES algorithms, with adjustments to accommodate the absence of stratospheric sounding spectral bands and to realize the advantage of greatly increased spatial resolution (1 km MODIS versus 17 km HIRS) with good radiometric signal to noise (better than 0.35 C for typical scene temperatures in all spectral bands).

In this document, we offer some background to the retrieval problem, review the MODIS instrument characteristics, describe the theoretical basis of the MODIS retrieval algorithm, discuss the practical aspects of the algorithm implementation, and outline the planned validation approach.

## 2. *Overview and background information*

This paper details the operational MODIS MOD07\_L2 algorithm for retrieving vertical profiles (soundings) of temperature and moisture, total column ozone burden, integrated total column precipitable water vapor, and several atmospheric stability indices. The MODIS atmospheric profile algorithm is a statistical regression with the option for a subsequent non-linear physical retrieval. The retrievals are performed using clear sky radiances measured by MODIS within a 5x5 field of view (approximately 5km resolution) over land and ocean for both day and night. A version of the algorithm using only the statistical regression is operational at the

Goddard Distributed Active Archive Center (GDAAC) processing system (<http://daac.gsfc.nasa.gov/MODIS>).

The methods presented here are based on the work of Li (2000), and work by Smith and Woolf (1988) and Hayden (1988). The clear advantage of MODIS for retrieving atmospheric profiles is its combination of fifteen infrared spectral channels suitable for sounding and high spatial resolution suitable for imaging (1 km at nadir). Temperature and moisture profiles at MODIS spatial resolution are required by a number of other MODIS investigators, including those developing sea surface temperature and land surface temperature retrieval algorithms. Total ozone and precipitable water vapor estimates at MODIS resolution are required by MODIS investigators developing atmospheric correction algorithms. The combination of high spatial resolution sounding data from MODIS, and high spectral resolution sounding data from AIRS, will provide a wealth of new information on atmospheric structure in clear skies.

## 2.1 *History*

Inference of atmospheric temperature profiles from satellite observations of thermal infrared emission was first suggested by King (1956). In this pioneering paper, King pointed out that the angular radiance (intensity) distribution is the Laplace transform of the Planck intensity distribution as a function of the optical depth, and illustrated the feasibility of deriving the temperature profile from the satellite intensity scan measurements. Kaplan (1959) advanced the temperature sounding concept by demonstrating that vertical resolution of the temperature field could be inferred from the spectral distribution of atmospheric emission. Kaplan noted that observations in the wings of a spectral band sense deeper regions of the atmosphere, whereas observations in the band center see only the very top layer of the atmosphere, since the radiation mean free path is small. Thus by properly selecting a set of sounding spectral channels at different wavelengths, the observed radiances could be used to make an interpretation of the vertical temperature distribution in the atmosphere.

Wark (1961) proposed a satellite vertical sounding program to measure atmospheric temperature profiles, and the first satellite sounding instrument (SIRS-A) was launched on NIMBUS-3 in 1969 (Wark and Hilleary, 1970). Successive experimental instruments on the NIMBUS series of polar orbiting satellites led to the development of the TIROS-N series of



operational polar-orbiting satellites in 1978. These satellites introduced the TIROS Operational Vertical Sounder (TOVS, Smith et al. 1979), consisting of the High-resolution Infrared Radiation Sounder (HIRS), the Microwave Sounding Unit (MSU), and the Stratospheric Sounding Unit (SSU). This same series of instruments continues to fly today on the NOAA operational polar orbiting satellites. HIRS provides 17 km spatial resolution at nadir with 19 infrared sounding channels. The first sounding instrument in geostationary orbit was the GOES VISSR Atmospheric Sounder (VAS, Smith et al. 1981) launched in 1980. The current generation GOES-8 sounder (Menzel and Purdom, 1994) provides 8 km spatial resolution with 18 infrared sounding channels; the GOES retrieval algorithm is detailed in Ma et al. (1999). An excellent review of the history of satellite temperature and moisture profiling is provided by Smith (1991).

## 2.2 Instrument Characteristics

MODIS is a scanning spectroradiometer with 36 spectral bands between 0.645 and 14.235  $\mu\text{m}$  (King et al. 1992). Table 1 summarizes the MODIS technical specifications.

**Table 1:** MODIS Technical Specifications

Orbit:	705 km altitude, sun-synchronous, 10:30 a.m. descending node
Scan Rate:	20.3 rpm, cross track
Swath Dimensions:	2330 km (cross track) by 10 km (along track at nadir)
Quantization:	12 bits
Spatial Resolution:	250 m (bands 1-2), 500 m (bands 3-7), 1000 m (bands 8-36)

Table 2 shows the MODIS spectral bands that are used in the MODIS algorithm. Note that in most cases the predicted (goal) noise is expected to be better than the specification. The data rate with 12 bit digitization and a 100% duty cycle is expected to be approximately  $5.1 \times 10^6$  bits/sec (55 Gbytes/day).

**Table 2: MODIS Spectral Band Specifications**

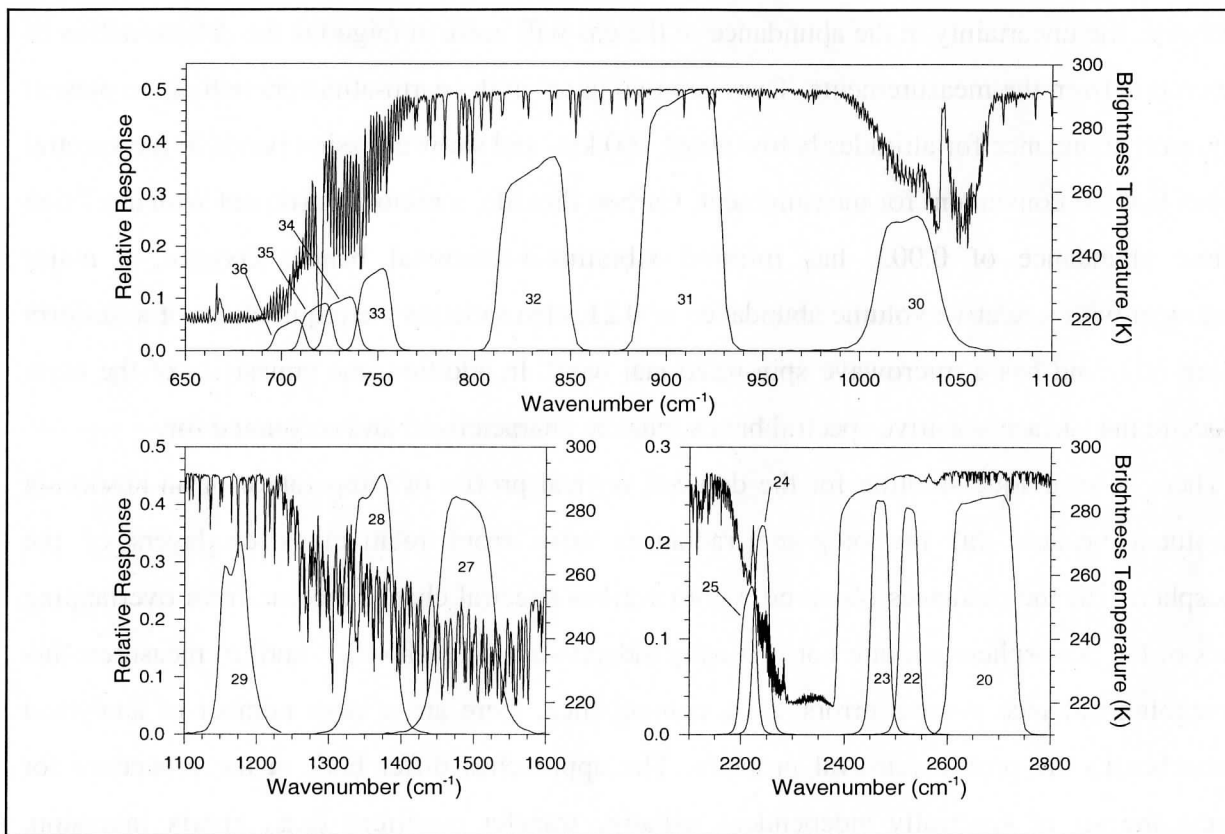
Primary Atmospheric Application	Band	Bandwidth <sup>1</sup>	T <sub>typical</sub> (K)	Radiance <sup>2</sup> at T <sub>typical</sub>	NEΔT (K) Specification	NEΔT (K) Predicted
Temperature profile	24	4.433-4.498	250	0.17	0.25	0.15
	25	4.482-4.549	275	0.59	0.25	0.10
Moisture profile	27	6.535-6.895	240	1.16	0.25	0.05
	28	7.175-7.475	250	2.18	0.25	0.05
	29	8.400-8.700	300	9.58	0.05	0.05
Ozone	30	9.580-9.880	250	3.69	0.25	0.05
Surface Temperature	31	10.780-11.280	300	9.55	0.05	0.05
	32	11.770-12.270	300	8.94	0.05	0.05
Temperature profile	33	13.185-13.485	260	4.52	0.25	0.15
	34	13.485-13.785	250	3.76	0.25	0.20
	35	13.785-14.085	240	3.11	0.25	0.25
	36	14.085-14.385	220	2.08	0.35	0.35

<sup>1</sup>  $\mu\text{m}$  at 50% response

<sup>2</sup>  $\text{W m}^{-2} \text{sr}^{-1} \mu\text{m}^{-1}$

Figure 1 shows the spectral responses of the MODIS infrared bands in relation to an atmospheric emission spectrum computed by a line-by-line radiative transfer model (LBL-RTM) for the US standard atmosphere.

**Figure 1:** MODIS infrared spectral response. Nadir viewing emission spectrum of U.S. Standard Atmosphere from LBL-RTM.



### 3. *Algorithm Description*

In section we describe the theoretical basis and practical implementation of the atmospheric profile retrieval algorithm.

#### 3.1 *Theoretical Background*

In order for atmospheric temperature to be inferred from measurements of thermal emission, the source of emission must be a relatively abundant gas of known and uniform distribution. Otherwise, the uncertainty in the abundance of the gas will make ambiguous the determination of temperature from the measurements. There are two gases in the earth-atmosphere that are present in uniform abundance for altitudes below about 100 km, and show emission bands in the spectral regions that are convenient for measurement. Carbon dioxide, a minor constituent with a relative volume abundance of 0.003, has infrared vibrational-rotational bands. Oxygen, a major constituent with a relative volume abundance of 0.21, also satisfies the requirement of a uniform mixing ratio and has a microwave spin-rotational band. In addition, the emissivity of the earth surface in the surface sensitive spectral bands must be characterized and accounted for.

There is no unique solution for the detailed vertical profile of temperature or an absorbing constituent because (a) the outgoing radiances arise from relatively deep layers of the atmosphere, (b) the radiances observed within various spectral channels come from overlapping layers of the atmosphere and are not vertically independent of each other, and (c) measurements of outgoing radiance possess errors. As a consequence, there are a large number of analytical approaches to the profile retrieval problem. The approaches differ both in the procedure for solving the set of spectrally independent radiative transfer equations (e.g., matrix inversion, numerical iteration) and in the type of ancillary data used to constrain the solution to insure a meteorologically meaningful result (e.g., the use of atmospheric covariance statistics as opposed to the use of an a priori estimate of the profile structure). There are some excellent papers in the literature which review the retrieval theory which has been developed over the past few decades (Fleming and Smith, 1971; Fritz et al., 1972; Rodgers, 1976; Twomey, 1977; and Houghton et al. 1984). The following sections present the mathematical basis for two of the procedures which have been utilized in the operational retrieval of atmospheric profiles from satellite measurements.

### 3.2 Statistical Regression Profile Retrieval

A computationally efficient method for determining temperature and moisture profiles from satellite sounding measurements uses previously determined statistical relationships between observed (or modeled) radiances and the corresponding atmospheric profiles. This method is often used to generate a first-guess for a physical retrieval algorithm, as is done in the International TOVS Processing Package (ITPP, Smith et al., 1993). The statistical regression algorithm for atmospheric temperature is described in detail in Smith et. al. (1970), and can be summarized as follows (the algorithm for moisture profiles is formulated similarly). In cloud-free skies, the radiation received at the top of the atmosphere at frequency  $\nu$  is the sum of the radiance contributions from the Earth's surface and from all levels in the atmosphere,

$$R(\nu_j) = \sum_{i=1}^N B[\nu_j, T(p_i)] w(\nu_j, p_i) \quad (1)$$

where

$w(\nu_j, p_i) = \epsilon(\nu_j, p_i) \tau(\nu_j, 0 \rightarrow p_i)$  is the weighting function,

$B[\nu_j, T(p_i)]$  is the Planck radiance for pressure level  $i$  at temperature  $T$ ,

$\epsilon(\nu_j, p_i)$  is the spectral emissivity of the emitting medium at pressure level  $i$ ,

$\tau(\nu_j, 0 \rightarrow p_i)$  is the spectral transmittance of the atmosphere above pressure level  $i$ .

The problem is to determine the temperature (and moisture) at  $N$  levels in the atmosphere from  $M$  radiance observations. However because the weighting functions are broad and represent an average radiance contribution from a layer, the  $M$  radiance observations are interdependent, and hence there is no unique solution. Furthermore, the solution is unstable in that small errors in the radiance observations produce large errors in the temperature profile. For this reason, the solution is approximated in a linearized form. First (1) is re-written in terms of a deviation from an initial state,

$$R(\nu_j) - R_0(\nu_j) = \sum_{i=1}^N \{B[\nu_j, T(p_i)] - B[\nu_j, T_0(p_i)]\} w(\nu_j, p_i) + e(\nu_j) \quad (2)$$

where

$e(\nu_j)$  is the measurement error for the radiance observation.

In order to solve (2) for the temperature profile  $T$  it is necessary to linearize the Planck function dependence on frequency. This can be achieved since in the infrared region the Planck function is much more dependent on temperature than frequency. Thus the general inverse solution of (2) for the temperature profile can be written as

$$T(p_i) - T_0(p_i) = \sum_{j=1}^M A(\nu_j, p_i) [R(\nu_j) - R_0(\nu_j)] \quad (3)$$

or in matrix form

$$T = AR$$

where  $A(\nu_j, p_i)$  is a linear operator. Referring back to (2), it can be seen that in theory  $A$  is simply the inverse of the weighting function matrix. However in practice the inverse is numerically unstable.

The statistical regression algorithm seeks a “best-fit” operator matrix  $A$  that is computed using least squares methods by utilizing a large sample of atmospheric temperature and moisture soundings, and collocated radiance observations. That is, we seek to minimize the error

$$\frac{\partial}{\partial A} |AR - T|^2 = 0$$

which is solved by the normal equations to yield

$$A = (R^T R)^{-1} R^T T \quad (5)$$

where

$(R^T R)$  is the covariance of the radiance observations,

$(R^T T)$  is the covariance of the radiance observations with the temperature profile.

Ideally, the radiance observations would be taken from actual MODIS measurements and used with time and space co-located radiosonde profiles to directly derive the regression coefficients  $A$ . In such an approach, the regression relationship would not involve any radiative transfer calculations. However, radiosondes are routinely launched only two times each day at 0000 UTC and 1200 UTC simultaneously around the earth; Terra passes occur at roughly 1100-1200 AM and 1000-1100 PM local standard time each day. It is therefore not possible to obtain many time and space co-located MODIS radiances. Alternatively, the regression coefficients can also be generated from MODIS radiances calculated using a transmittance model with profile input from

a global temperature and moisture radiosonde database. In this approach, the accuracy of the atmospheric transmittance functions for the various spectral bands is crucial for accurate parameter retrieval.

In the regression procedure, the primary predictors are MODIS infrared spectral band brightness temperatures. The algorithm uses 12 infrared bands with wavelengths between  $4.465\mu\text{m}$  and  $14.235\mu\text{m}$ . Surface emissivity effects in the short wave window bands are mitigated by regressing against band differences (e.g., instead of  $\text{BT}(4.5\mu\text{m})$  and  $\text{BT}(4.4\mu\text{m})$  we use the difference,  $\text{BT}(4.5\mu\text{m}) - \text{BT}(4.4\mu\text{m})$  in the regression, where BT represents brightness temperature). Estimates of surface pressure are also used as predictors to improve the retrieval. Table 3 lists the predictors and their noise used in the regression procedure. Quadratic terms of all brightness temperatures in Table 3 are also used as predictors to account for the moisture non-linearity in the MODIS radiances. The noise used in the algorithm is larger than estimates of post-launch detector noise in order to account for variability between the ten detectors (striping). The regression coefficients are generated for 680 local zenith angles from nadir to  $65^\circ$ , and various IR emissivity spectra are assigned to the training profiles to account for varying surface properties in the regression procedure.

**Table 3:** Predictors and their uncertainty used in the regression procedure

Predictor	Noise used in MOD07 algorithm	Post-launch NEdT averaged over detectors
Band 25-24 BT ( $4.47 - 4.52\mu\text{m}$ )	$0.75^\circ\text{K}$	$0.163^\circ\text{K}$ (band 24) $0.086^\circ\text{K}$ (band 25)
Band 27 BT ( $6.7\mu\text{m}$ )	$0.75^\circ\text{K}$	$0.376^\circ\text{K}$
Band 28 BT ( $7.3\mu\text{m}$ )	$0.75^\circ\text{K}$	$0.193^\circ\text{K}$
Band 29 BT ( $8.55\mu\text{m}$ )	$0.189^\circ\text{K}$	$0.189^\circ\text{K}$
Band 30 BT ( $9.73\mu\text{m}$ )	$0.75^\circ\text{K}$	$0.241^\circ\text{K}$
Band 31 BT ( $11\mu\text{m}$ )	$0.167^\circ\text{K}$	$0.167^\circ\text{K}$
Band 32 BT ( $12\mu\text{m}$ )	$0.192^\circ\text{K}$	$0.192^\circ\text{K}$
Band 33 BT ( $13.3\mu\text{m}$ )	$0.75^\circ\text{K}$	$0.308^\circ\text{K}$



Band 34 BT (13.6 $\mu$ m)	0.75 $^{\circ}$ K	0.379 $^{\circ}$ K
Band 35 BT (13.9 $\mu$ m)	0.75 $^{\circ}$ K	0.366 $^{\circ}$ K
Band 36 BT (14.2 $\mu$ m)	1.05 $^{\circ}$ K	0.586 $^{\circ}$ K
Surface Pressure	5 hPa	--
Latitude	0.001 $^{\circ}$	--

In the MODIS retrieval algorithm, more than 8400 global radiosonde profiles of temperature, moisture, and ozone from an extension of the NOAA-88b data set are used in the calculations. The radiative transfer calculation of the MODIS spectral band radiances is performed with the PFAAST model for each profile from the training data set to provide a temperature-moisture-ozone profile/MODIS radiance pair. Estimates of the MODIS instrument noise is added into the calculated spectral band radiances. The regression coefficients are then generated using these calculated radiances and the matching atmospheric profile. To perform the regression, Eq.(5) can be applied to the actual MODIS measurements to obtain the estimated atmospheric profiles; integration yields the total precipitable water or total column ozone. The advantage of this approach is that it does not need MODIS radiances collocated in time and space with atmospheric profile data, it requires only historical profile observations. However, it involves the radiative transfer calculations and requires an accurate forward model in order to obtain a reliable regression relationship. Any uncertainties (e.g., a bias of the forward model) in the radiative calculations will influence the retrieval. To address model uncertainties, radiance bias adjustments have been implemented in the retrieval algorithm.

### **3.3 Physical Profile Retrieval**

The statistical regression algorithm has the advantage of computational efficiency, numerical stability, and simplicity. However, it does not account for the physical properties of the radiative transfer equation (RTE). After computing atmospheric profiles from the regression technique, a non-linear iterative physical algorithm (Li et al., 2000) applied to the RTE often improves the solution. The physical retrieval approach is described in this section.

The physical procedure is based on the regularization method (Li et al., 2000) by minimizing the penalty function defined by



$$Y(X) = \|Y^m - Y(X)\|^2 + \gamma \|X - X_0\|^2 \quad (6)$$

to measure the degree of fit of the MODIS spectral band measurements to the regression first guess. In equation 6,  $X$  is the atmospheric profile to be retrieved,  $X_0$  is the initial state of the atmospheric profile or the first guess from regression,  $Y^m$  is the vector of the observed MODIS brightness temperatures used in the retrieval process,  $Y(X)$  is the vector of calculated MODIS brightness temperatures from an atmospheric state ( $X$ ), and  $\gamma$  is the regularization parameter that can be determined by the Discrepancy Principle (Li and Haung, 1999; Li et al. 2000). The solution provides a balance between MODIS spectral band radiances and the first guess. If a radiative transfer calculation using the first guess profile as input fits all the MODIS spectral band radiances well, less weight is given to the MODIS measurements in the non-linear iteration, and the solution will be only a slight modification of the first guess. However, if the first guess does not agree well with the MODIS spectral band radiances, then the iterative physically retrieved profile will be given a larger weight. Thus, the temperature, moisture, and ozone profiles as well as the surface skin temperature will be modified in order to obtain the best simultaneous fit to all the MODIS spectral bands used. For more details, see Li et al. (2000).

### ***3.4 Derived Products***

#### ***3.4.1 Total column precipitable water vapor and ozone***

Determination of the total column precipitable water vapor and total ozone is performed by integrating moisture and ozone profiles through the atmospheric column. The total column precipitable water vapor “Water\_Vapor” parameter included in the MODIS MOD07\_L2 data is integrated from the 101-level retrieved mixing ratio profiles. Atmospheric profile retrievals are saved at only 20 levels in the MOD07 data so integration by the user of the 20-level profiles may not result in the same value reported in the “Water\_Vapor” field. Another total column water vapor parameter, “Water\_Vapor\_Direct” is obtained by direct regression from the integrated moisture in the training data.

### 3.4.2 Atmospheric Stability

One measure of the thermodynamic stability of the atmosphere is the total-totals index, defined by

$$TT = T_{850} + TD_{850} - 2T_{500}$$

where  $T_{850}$  and  $T_{500}$  are the temperatures at the 850 mb and 500 mb levels, respectively, and  $TD_{850}$  is the 850-mb level dew point.  $TT$  is traditionally estimated from radiosonde point values. For a warm moist atmosphere underlying cold mid-tropospheric air,  $TT$  is high (e.g., 50-60 K) and intense convection can be expected. There are two limitations of radiosonde derived  $TT$ : (a) the spacing of the data is too large to isolate local regions of probable convection and (b) the data are not timely since they are available only twice per day.

If we define the dew point depression at 850 mb,  $D_{850} = T_{850} - TD_{850}$ , then

$$TT = 2(T_{850} - T_{500}) - D_{850}$$

Although point values of temperature and dew point cannot be observed by satellite, the layer quantities observed can be used to estimate the temperature lapse rate of the lower troposphere ( $T_{850} - T_{500}$ ) and the low level relative moisture concentration  $D_{850}$ . Assuming a constant lapse rate of temperature between the 850 and 200 mb pressure levels and also assuming that the dew point depression is proportional to the logarithm of relative humidity, it can be shown from the hydrostatic equation that

$$TT = 0.1489DZ_{850-500} - 0.0546DZ_{850-200} + 16.03\ln(RH)$$

where  $DZ$  is the geopotential thickness in meters and  $RH$  is the lower tropospheric relative humidity, both estimated from the MODIS radiance measurements as explained earlier.

Smith and Zhou (1982) reported several case studies using this approach. They found general agreement in gradients in space and time, with the satellite data providing much more spatial detail than the sparse radiosonde observations.

Another estimate of atmospheric stability is the lifted index, which can be derived from the MODIS determined temperature and moisture profile. The lifted index is the difference of the measured 500 mb temperature and the temperature calculated by lifting a surface parcel dry adiabatically to its local condensation level and then moist adiabatically to 500 mb. As this value goes negative it indicates increased atmospheric instability.

#### **4.0 Operational Retrieval Implementation**

The operational MODIS retrieval algorithm consists of several procedures that include cloud detection, averaging clear radiances from 5 by 5 field-of-view (FOV) areas, bias adjustment of MODIS brightness temperatures for forward model and instrument, regression retrieval, and an option to perform a physical retrieval. Because of computer limitations, the MODIS MOD07\_L2 retrieval algorithm that is operational at GDAAC processing system includes only the regression retrieval. A version of the algorithm with the physical retrieval will be available for MODIS direct broadcast processing as part of the International MODIS/AIRS Processing Package (IMAPP) developed at the Space Science and Engineering Center (SSEC) at the University of Wisconsin-Madison (<http://cimss.ssec.wisc.edu/~gumley/IMAPP/IMAPP.html>). The radiative transfer calculation of the MODIS spectral band radiances is performed using a transmittance model called Pressure layer Fast Algorithm for Atmospheric Transmittances (PFAAST) (Eyre and Woolf 1988, Hannon et al. 1996); this model has 101 pressure level vertical coordinates from 0.05 to 1100 hPa. The calculations take into account the satellite zenith angle, absorption by well-mixed gases (including nitrogen, oxygen, and carbon dioxide), water vapor (including the water vapor continuum), and ozone.

#### **4.1 Cloud detection algorithm**

MODIS atmospheric and surface parameter retrievals require clear sky measurements. The operational MODIS cloud mask algorithm (Ackerman et al. 1998) is used to identify pixels that are cloud free. The MODIS cloud mask algorithm determines if a given pixel is clear by combining the results of several spectral threshold tests. A confidence level of clear sky for each pixel is estimated based on a comparison between observed radiances and specified thresholds. The operational retrieval algorithm requires at least 5 of the 25 pixels in a 5x5 field-of-view area to have been assigned a 95% or greater confidence of clear by the cloud mask. The retrieval for each 5x5 field-of-view area is performed using the average radiance of those pixels that were considered clear. Since the decision to perform a retrieval depends on the validity of the cloud mask algorithm, cloud contamination may occur if the cloud mask fails to detect a cloud, or the retrieval may not be run if the cloud mask falsely identifies a cloud.

## 4.2 Radiance bias adjustment

The forward model-calculated radiances have biases with respect to the MODIS measured radiances. There are several possible causes including calibration errors, spectral response uncertainty, temperature and moisture profile inaccuracies, and forward model error. The statistical regression and the physical retrieval methods use both measured and calculated radiances and thus require that this bias be minimized. Techniques developed for computing GOES sounder radiance biases with respect to the forward model (Hayden 1988) were employed in the MODIS atmospheric profile algorithm. Bias adjustment for radiative transfer calculation of MODIS spectral band radiances is demonstrated to have a positive impact on the atmospheric product retrievals.

Radiance bias calculations are routinely computed for the SGP ARM-CART site for clear scenes with MODIS sensor zenith angle less than  $35^\circ$ . Observed MODIS radiances, averaged from a 5x5 field-of-view area, are compared with those computed by the same transmittance model used in the algorithm. The calculations of radiances are performed using the 101-level PFAAST model, with temperature and moisture profile input from National Center for Environmental Prediction's Global Data Analysis System (NCEP-GDAS) global analysis data. Skin temperature and emissivity estimates are from regression with MODIS radiances. To establish credibility for the regression-derived skin temperature input, actual observed skin temperature from a ground-based downward-looking infrared thermometer (IRT) that measures the radiating temperature of the ground surface (<http://www.arm.gov/docs/instruments/static/irt.html>) was also used. Figure 6 shows that, on average over 60 clear-sky day and night cases from April 2001 to June 2002, the biases computed using the regression-based skin temperature differ very little from those computed using the IRT skin temperature.

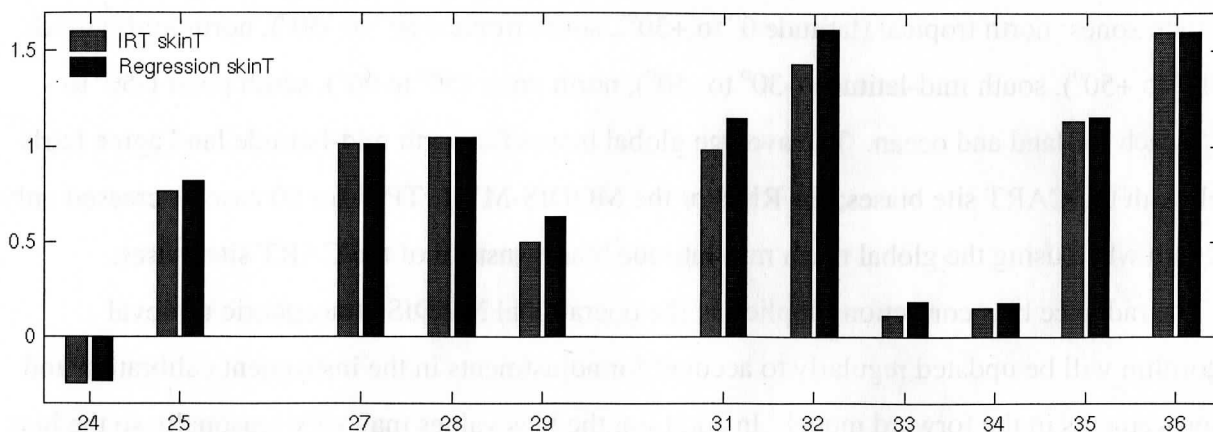


**Figure 6:** Average (Observed-Calculated) brightness temperature for MODIS IR bands 24, 25, 27-29, and 31-36 from 60 clear sky cases at the SGP ARM-CART site from April 2001 to June 2002. Red bars indicate radiance calculations used skin temperature observed by the IRT; regression-derived skin temperature was used for the calculated radiances in the blue bars.

A comparison of MODIS products at the SGP ARM-CART site with and without the bias correction (not shown) confirms a significant improvement with the bias corrections. The RMS for the CART site MWR minus MODIS decreased from 4.94 mm to 3.61 mm when the bias corrections were applied. The improvements were primarily apparent for moist cases where the bias correction helped to correct a dry bias. Because the MODIS retrieval algorithm is applied globally, the biases computed at the SGP ARM-CART site are not appropriate for application at other latitudes and for other ecosystem types. Thus, biases have been computed for other regions of the globe; however, they are less well validated. Future versions of the algorithm will include a more advanced global bias scheme that uses a regression based on air-mass predictors (atmospheric layer thickness, surface skin temperature, and TPW) such as that employed on the TIROS Operational Vertical Sounder (TOVS) (Eyre 1992; Harris and Kelly, 2001).

To compute the global radiance biases, observed MODIS brightness temperatures were compared with calculated brightness for 270 clear-sky scenes from June 2 - 5, 2001 with MODIS viewing zenith angle  $< 30^\circ$ . Calculations of brightness temperatures were performed as outlined above with skin temperature estimated from regression of MODIS radiances. As there are known difficulties in retrieving skin temperature and emissivity over the desert, these cases were excluded from the global averages. The global biases are separated into twelve groups: six

latitude zones: north tropical (latitude  $0^{\circ}$  to  $+30^{\circ}$ ), south tropical ( $0^{\circ}$  to  $-30^{\circ}$ ), north mid-latitude ( $+30^{\circ}$  to  $+50^{\circ}$ ), south mid-latitude ( $-30^{\circ}$  to  $-50^{\circ}$ ), north polar ( $50^{\circ}$  to  $90^{\circ}$ ), south polar ( $-50^{\circ}$  to  $-90^{\circ}$ ), each for land and ocean. The average global biases for north mid-latitude land agree fairly well with the CART site biases; the RMS of the MODIS-MWR TPW for 60 cases increased only 0.2 mm when using the global north mid-latitude biases instead of the CART site biases.

The radiance bias corrections applied in the operational MODIS atmospheric retrieval algorithm will be updated regularly to account for adjustments in the instrument calibration and improvements in the forward model. In addition, the bias values may vary seasonally so the bias corrections calculated from four days in June may need to be updated.

#### **4.3 Adjustments to the NOAA-88b training data set**

The NOAA-88b data contains globally distributed radiosonde observations from all twelve months in 1988. Profiles of temperature and moisture and surface data from this data set were used to compute the regression coefficients for the MODIS statistical retrieval. To limit the retrievals to training data with physical relevance to the observed conditions, the NOAA-88b data was partitioned into seven zones based on the  $11\mu\text{m}$  brightness temperatures (BT11) calculated from the profiles. The seven zones are BT11  $< 245$ , 245-269, 269-285, 285-294, 294-300, 300-310, and  $> 310^{\circ}\text{K}$ . When each statistical retrieval is performed, it uses only the subset of the training data corresponding to BT11.

The original NOAA-88b training data set includes approximately 7500 globally distributed radiosonde profiles and surface data. After partitioning, there was insufficient training data for the very warm surfaces (the last two zones, BT11  $> 300^{\circ}\text{K}$ ). To address this problem, new radiosonde data from the north African desert regions for January – December 2001 were added to the training data set. 900 new radiosondes, spread equally through the twelve months, met the criteria of relative humidity  $< 90\%$  at each level and physically reasonable behavior up to 100hPa; profiles of temperature and moisture from these radiosondes were added to the NOAA-88b data set. Partitioning the BT11 into seven zones and adding training data improves the MODIS TPW retrievals; the most significant improvements occur for scenes with BT11 in the two highest classes.



#### 4.4 Surface emissivity for IR 4.5 $\mu\text{m}$ spectral bands

The infrared surface emissivity in the NOAA-88b training data is variable for different atmospheric profiles, with a mean of 0.95 for longwave IR bands (9 – 13  $\mu\text{m}$  bands) and 0.85 for shortwave IR bands; the standard deviation is 0.05 for both longwave and shortwave. In most situations the training data set accounts for the global emissivity variations. However, for some regions such as the deserts of north Africa, the surface emissivity has the potential to be significantly lower at 4  $\mu\text{m}$  than at 11  $\mu\text{m}$  (Salisbury and D’Aria 1992). Because desert emissivities are not included in the training data set, the IR 4.4  $\mu\text{m}$  and 4.5  $\mu\text{m}$  (bands 24 and 25) were not accurately represented and the MODIS retrievals were excessively moist in the desert regions. To remedy this problem, the difference between these two bands is used as a single predictor instead of using bands 24 and 25 independently; this subtraction removes most of the surface emissivity signal in the regression equation. Brightness temperature increments for band 24, band 25, and the difference band 25 – band 24 with respect to emissivity are shown in Figure 7. The BT difference between band 25 and band 24 is found to be much less sensitive to the surface emissivity change than the BT of either band 24 or band 25 independently.

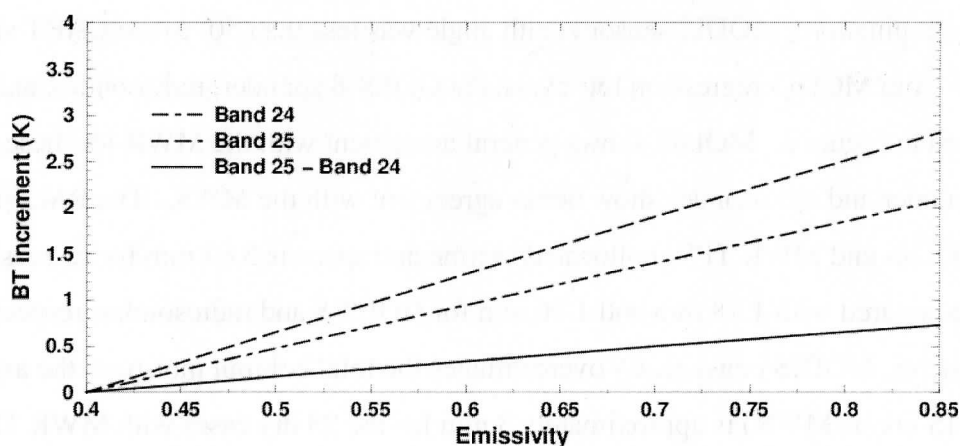


**Figure 7:** Brightness temperature increment ( $^{\circ}\text{K}$ ) for bands 24 and 25 individually (dash-dot and dash, respectively) and for the difference between bands 25-24 (solid line). Calculations used a standard U.S. mid-latitude summer atmosphere.

#### 5. Validation of MODIS MOD07 products

Atmospheric retrievals from MODIS have been compared with those from observing systems have been compared at three spatial scales: a) a fixed point with ground-based measurements

(SGP ARM-CART), b) the continental scale with GOES sounder products, and c) the global scale with retrievals from the Special Sensor Microwave/Imager (SSM/I) and Total Ozone Mapping Spectrometer (TOMS).

### **5.1 Comparison of MODIS temperature and moisture with ARM-CART observations**

Specialized instrumentation at the Southern Great Plains (SGP) Atmospheric Radiation Measurement-Cloud and Radiation Testbed (ARM-CART) in Oklahoma facilitates comparisons of MODIS atmospheric products with other observations collocated in time and space. Terra passes over the SGP CART daily between 0415-0515 UTC and 1700-1800 UTC. Radiosondes are launched three times each day at approximately 0530, 1730, and 2330 UTC. Observations of total column moisture are made by the microwave water radiometer (MWR) every 40-60 seconds. An additional comparison is possible with the GOES-8 sounder (Menzel and Purdom 1994; Menzel et al. 1998) that retrieves TPW hourly.

MODIS retrieved products were compared for 64 clear-sky cases from April 2001 to June 2002. Manual inspection of visible and infrared images excluded any scenes with the possibility of cloud contamination. MODIS sensor zenith angle was less than  $50^\circ$  to the CART site for all cases. TPW from MODIS regression retrievals, the GOES-8 sounder, radiosondes, and the MWR are compared in Figure 8. MODIS shows general agreement with the MWR for these cases; GOES-8 sounder and radiosondes show better agreement with the MWR. The RMS difference between MODIS and MWR TPW collocated in time and space is 3.63 mm for regression retrievals, compared with 1.78 mm and 1.16 mm for GOES-8 and radiosondes, respectively. For dry atmospheres, MODIS consistently overestimates the total column moisture; the average TPW bias (MODIS minus MWR) is approximately 3 mm for the 25 dry cases with MWR TPW less than 10 mm.



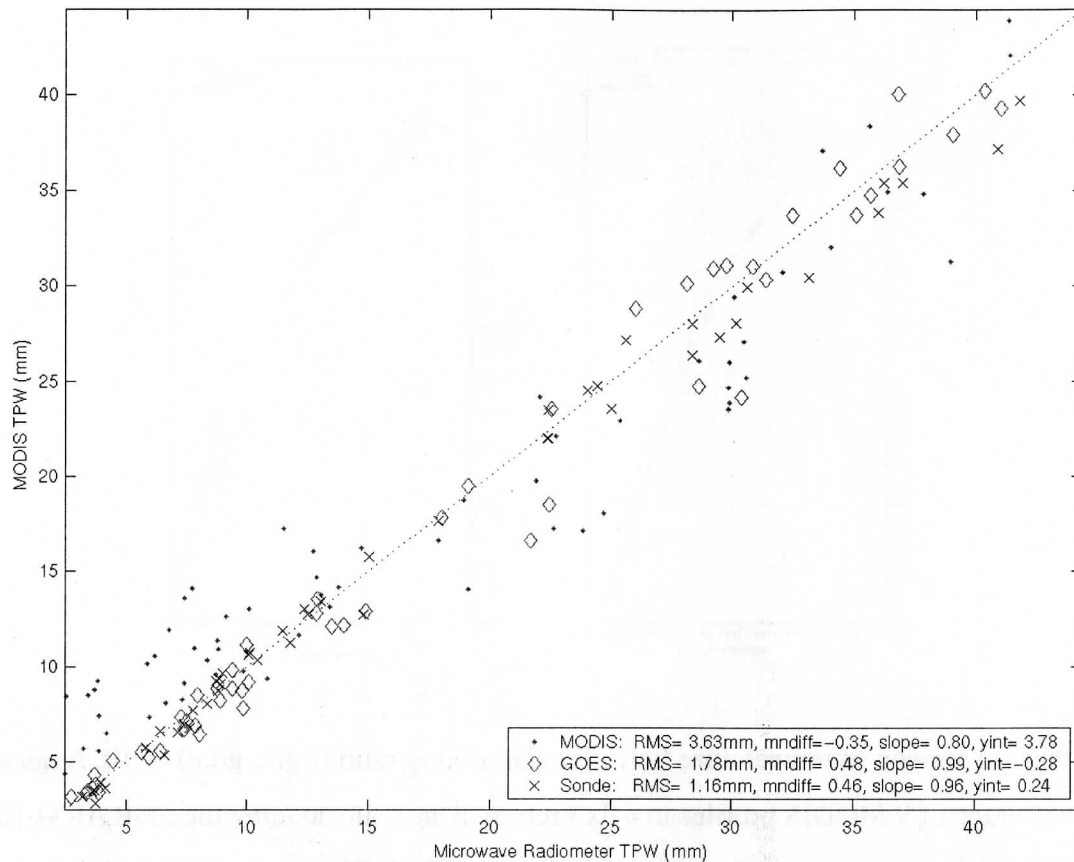


**Figure 8.** Comparison of TPW from MODIS regression (red dot), GOES-8 (blue diamonds), and radiosonde (black cross) with the SGP ARM-CART microwave water radiometer (MWR) in millimeters. 64 cases from 01 April 2001 to June 2002 are shown in the comparison. The dotted line indicates a one-to-one correspondence.

An example comparison of RAOB and MODIS temperature and moisture is shown in Figure 9. For atmospheres with fairly monotonic, smooth temperature and moisture distribution, MODIS retrievals compare well to radiosondes. However, in situations with isolated layers of sharply changing temperature or moisture, MODIS is not able to capture the finer-scale structure. Improved sounding capability is expected from the Atmospheric Infrared Sounder (AIRS) on Aqua.

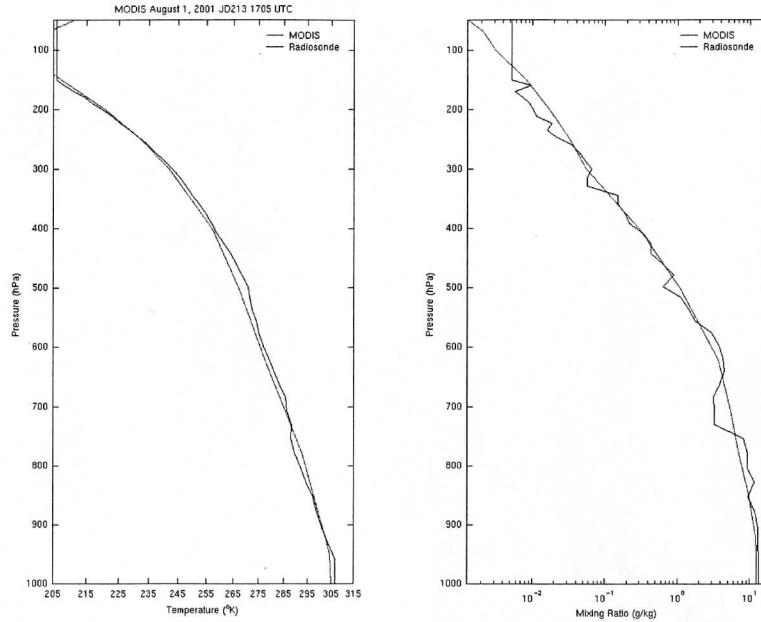


**Figure 9.** Comparison of temperature (left, °K) and mixing ratio (right, g/kg) on 01 August 2001 from the average of 9 MODIS profiles in a 3x3 retrieval area surrounding the SGP ARM-CART site at 1705 UTC (blue), and a radiosonde launched at 1728 UTC (black). In this situation where the temperature and moisture profiles are smooth, MODIS captures the vertical structure fairly well.

## 5.2 Continental-Scale comparisons between MODIS and GOES TPW

On the continental-scale, MODIS TPW was compared to GOES-8 and GOES-10 sounder retrievals of TPW over the continental United States and Mexico. GOES TPW has been well validated (Schmit et al. 2002). GOES has a resolution at the sub-satellite point of 10km and uses radiances measured from a 3 by 3 field of view area (approximately 30 km resolution) to retrieve one atmospheric profile, while MODIS has nadir resolution of 1km and uses a 5 by 5 field of view area (5 km resolution). Unlike the MODIS retrieval, GOES hourly radiance measurements are supplemented with hourly surface temperature and moisture observations as additional information in the GOES retrieval. MODIS and GOES retrieval procedures also use different first guess profiles; GOES uses a numerical model forecast, while MODIS uses the previously described regression retrieval.

Figure 10 compares MODIS TPW to TPW retrieved by the GOES-8 and GOES-10 sounders over North America for 02 June 2001 during the day and at night. The two show fairly good agreement except the MODIS TPW retrieved by regression is drier than GOES over Oklahoma, Arkansas, and the Gulf of Mexico. TPW retrieved by physical retrieval shows better agreement with GOES in these areas.

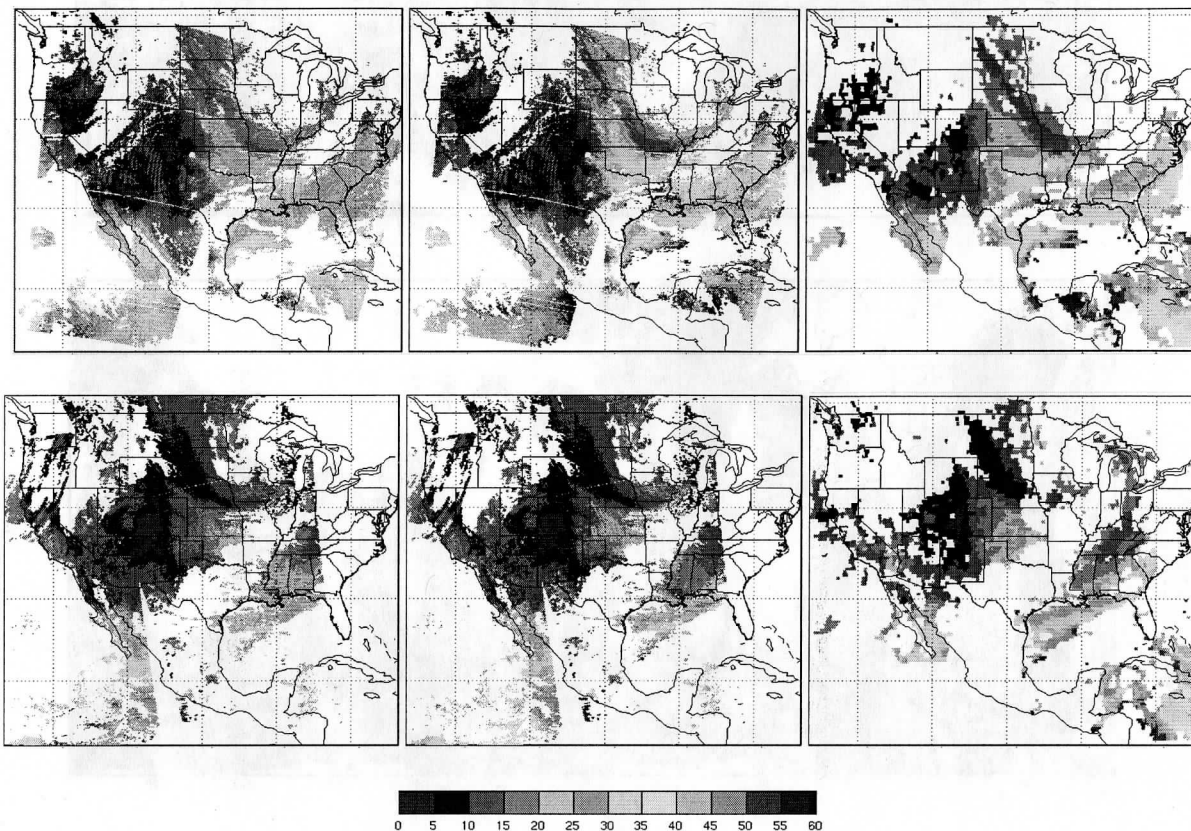


**Figure 10.** Total precipitable water (mm) for 02 June 2001 over North America retrieved by MODIS regression (left), MODIS physical (center), and GOES-8 and GOES-10 (combined, right). The top column shows daytime retrievals (4 MODIS granules from 1640, 1645, 1820, 1825 UTC; GOES at 1800UTC), and the bottom column nighttime (MODIS 0435, 0440, 0445, 0615, 0620 UTC; GOES 06 UTC).

### 5.3 Global comparisons of MODIS products with SSM/I and TOMS

Global TPW from MODIS atmospheric retrievals is compared with TPW from the Defense Meteorological Satellite Program (DMSP) SSM/I (Alishouse, 1990; Ferraro, 1996; Wentz, 1997) for 22 May 2002 in Figure 11.

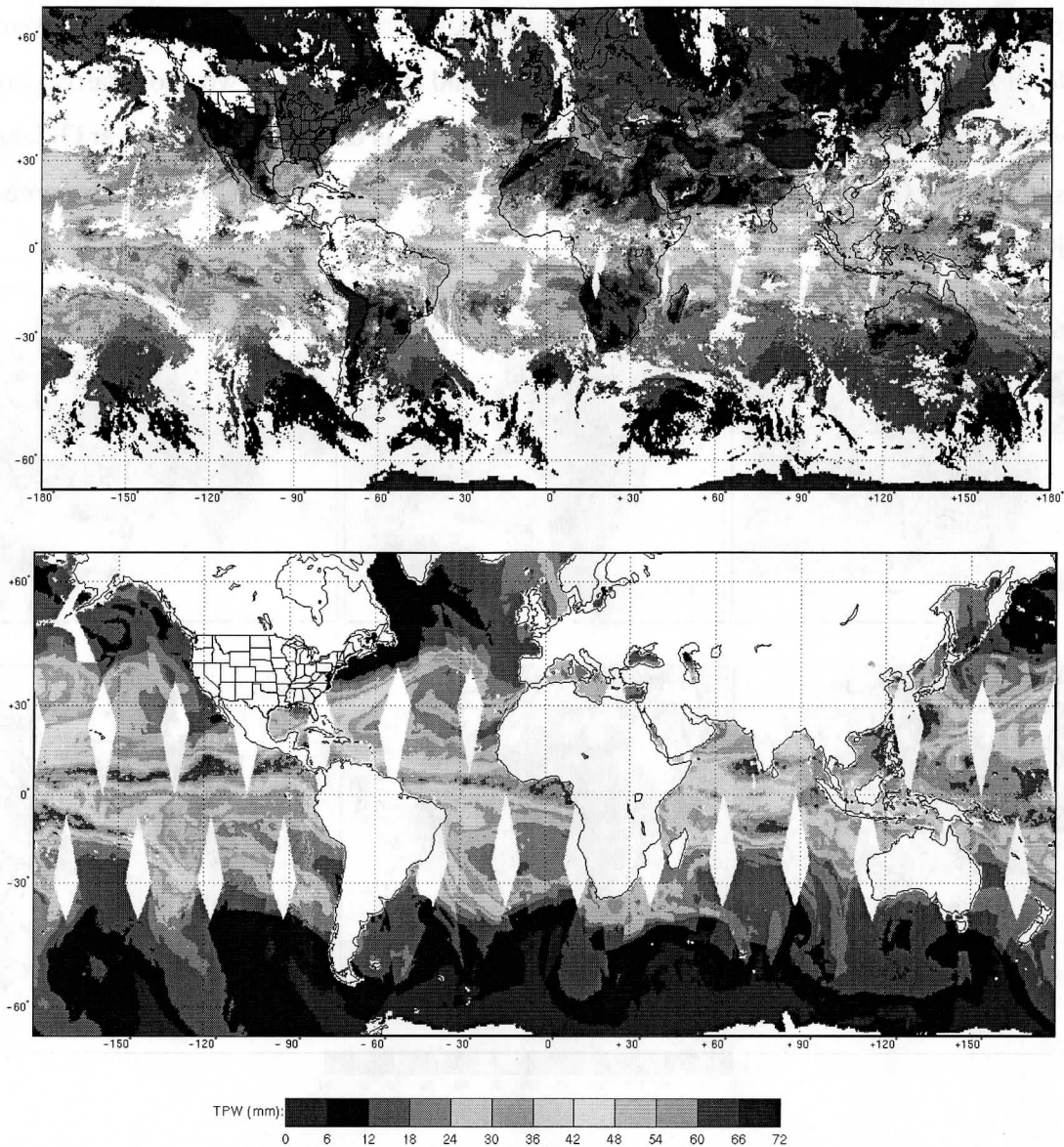


**Figure 11.** MODIS TPW (mm, upper panel) and SSM/I f-14 TPW (mm, lower panel) distribution on 22 May 2002. Retrievals from ascending and descending passes were averaged to obtain these values. The color scale is the same for both MODIS and SSM/I and is shown below the two images. SSM/I data were obtained through <http://www.ssmi.com>. MODIS data was degraded to 25 km resolution from the original 5 km resolution for this figure.

The SSM/I (resolution 12.5 km) retrieves products for clear or cloudy skies over ocean only and uses the 22 and 37 GHz microwave channels. MODIS and SSM/I show similar patterns of TPW distribution and similar magnitudes, however MODIS retrievals are somewhat less moist over

tropical oceans. Some of the differences can be attributed to the fact that MODIS does not retrieve cloudy pixels and, thus, does not capture the moist environment around clouds. This can affect the results even where MODIS retrievals were performed since the retrieval only requires that 5 of the 25 pixels in a 5x5 MODIS field-of-view area be clear. The remaining cloudy pixels are excluded, however the retrieval is still performed using only the clear pixels. Other differences may be attributed to the time differences between the two satellite overpasses.

MODIS total column ozone retrievals are compared with ozone from the NASA/GSFC Total Ozone Mapping Spectrometer (TOMS) (Bowman and Krueger 1985; McPeters et al. 1996, 1998) ozone measurements from the Earth Probe (EP) satellite for 22 May 2002 in Figure 12. The general distribution of ozone from TOMS is similar to that from MODIS. In order to predict the evolution of ozone on time scales of a few days to a week, reliable measurements of ozone distribution are needed. However, the TOMS instrument measures backscattered ultraviolet solar radiation and can not provide measurements at night. High spatial resolution IR radiance measurements at  $9.6\mu\text{m}$  from MODIS allow ozone estimates during both day and night.



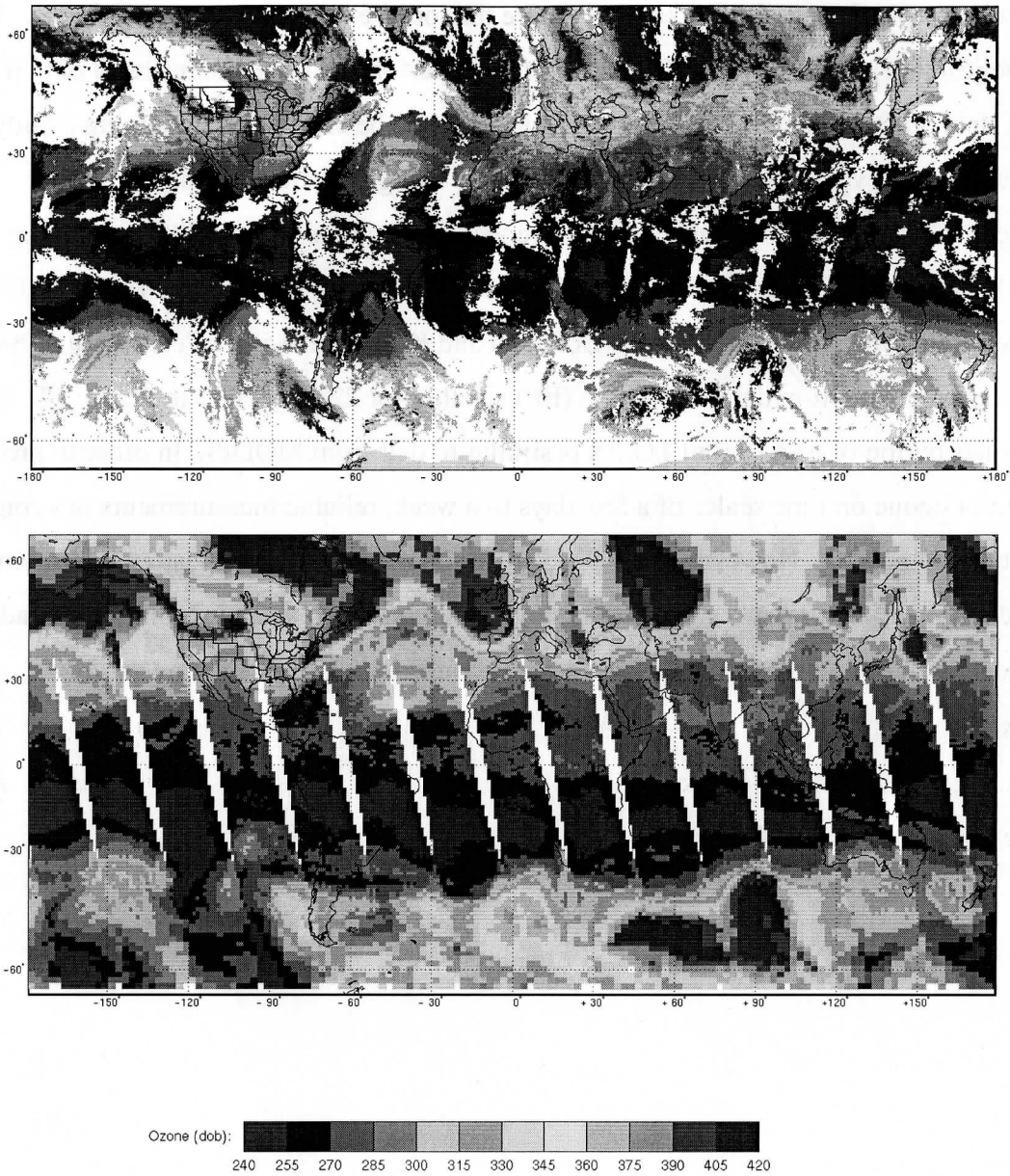


**Figure 12** Total column ozone (Dobson units) for 02 June 2001 for MODIS (top) and TOMS (bottom). TOMS data was obtained from <http://toms.gsfc.nasa.gov/ozone/ozone.html>.

## **6.0 Technical Issues**

Liam: please update section 6 or leave as is if current

### **6.1 Instrument Errors**

A complete error analysis including the effects of instrument calibration and noise as well as ancillary input data errors remains to be completed. The past performance of these algorithms with HIRS data is documented as temperature profiles errors at about 1.9 C, dewpoint temperature profile errors at about 4 C, total column ozone at about 10%, total column water vapor at about 10%, and gradients in atmospheric stability within 0.5 C.

The profile and total atmospheric column algorithms are based on HIRS experience. One significant difference between MODIS and HIRS is the absence of any stratospheric channels on MODIS (15.0, 14.7, and 14.5  $\mu\text{m}$ ). This will primarily affect the accuracy of the total ozone concentration estimates. The assumption for the MODIS algorithms presented here is that the slowly varying stratospheric temperatures are estimated very well by the forecast model. The higher spatial resolution of the MODIS compared to the HIRS will make clear sky radiance estimates more accurate and hence the RMS errors of the profile retrievals can be expected to improve (possibly by 0.5 C but exactly how much remains to be seen from actual data).

### **6.2 Data Processing Considerations**

Processing is to be accomplished globally at  $5\times 5$  pixel resolution in regions where a sufficient number of clear FOVs are available. Clear FOVs are averaged to reduce instrument single sample noise. An estimate of the processing requirements for this algorithm follows. Timing tests were conducted on a Silicon Graphics Power Indigo<sup>2</sup> (R8000/75 Mhz). The Version 1 MODIS atmospheric profiles code (statistical regression only) was run on simulated cloud-free MODIS Level 1B radiance data supplied by the MODIS Science Data Support Team. The input dataset contained 100 MODIS scans, which translates to 1000 along track 1 kilometer pixels. Processing was done on  $5\times 5$  blocks of pixels, and input data included the Level 1B radiances, corresponding geolocation data, simulated cloud mask data, and ancillary data (surface temperature and water vapor mixing ratio). The timing shown below reflects all phases of the processing, including

opening and reading input data files, computing retrieval parameters, and writing the output data file. Timing was measured using the Unix 'timex' command. Results are shown in Table 4.

**Table 4:** Timing test results for MODIS atmospheric profiles code (statistical regression)

Real	484.4 sec
User	134.2 sec
System	301.7 sec

### **6.3 Quality Control**

Quality control will be accomplished by manual and automatic inspection of the data and comparison to other sources of information. Automatic tests will check for physically realistic output values of temperature and moisture. Regional and global mean temperatures at 300, 500, and 700 mb will be monitored for weekly consistency; similarly dew point temperatures at 700 mb will be monitored. Global and regional precipitable water will also be tracked for spurious trends. Ozone in the polar regions will be averaged regionally and monitored for weekly consistency. Acceptable variations from week to week will be determined from the actual data.

### **6.4 Exception Handling**

The algorithm will check the validity of input radiances using metadata attached to the data itself, and validity tests developed post-launch. If the required input radiance data is bad, suspect, or not available, then the algorithm will record the output products as missing for that 5×5 pixel area.

### **6.5 Data Dependencies**

The profile retrieval algorithm requires calibrated, navigated, coregistered 1 km FOV radiances from channels 20 (3.75  $\mu\text{m}$  shortwave window), 22-25 (3.96 to 4.52  $\mu\text{m}$  shortwave CO<sub>2</sub> absorption band), 27-29 (6.72 to 8.55  $\mu\text{m}$  for moisture information), 30 (9.73  $\mu\text{m}$  for ozone), 31-32 (11.03 and 12.02 split window), and 33-36 (13.34, 13.64, 13.94, and 14.24  $\mu\text{m}$  CO<sub>2</sub> absorption band channels). The MODIS Cloud Mask will be also used for cloud screening, and for surface type determination (land or sea). The MODIS viewing angle for a given FOV



must be known. The NCEP global model estimates of surface temperature and pressure as well as profiles of temperature and moisture will be initially used in the calculation; as the AIRS/AMSU profiles become available, they will also be used.

## 6.6 Assumptions

The data are assumed to be calibrated (within the instrument noise), navigated (within one FOV), and coregistered (within two tenths of a FOV). The accuracy of the retrievals will depend on the on-orbit NEAT values in the infrared channels, estimates of which were shown in Table 2. It is assumed that high-quality global forecast model (e.g. NCEP, ECMWF, or GSFC/DAO) output or analysis fields will present for the derivation of first guess temperature and moisture profiles, since the retrieval algorithm essentially adjusts the guess just enough to fit the measured radiances.

## 6.7 Output Product Description

A single output file (MOD07) combining four products will be generated as part of the MODIS atmospheric profile retrieval algorithm; Table 4 lists the parameters and their units.

**Table 5:** Parameters included in products MOD30, MOD07, MOD38, MOD08

Resolution:  $5 \times 5$  pixel, Temporal sampling: Day and Night, Restrictions: Clear Sky only

TAI time at start of scan	(seconds since 1993-1-1 00:00:00.0 0)
Geodetic Latitude	(degrees_north)
Geodetic Longitude	(degrees_east)
Solar Zenith Angle, Cell to Sun	(degrees)
Solar Azimuth Angle, Cell to Sun	(degrees)
Sensor Zenith Angle, Cell to Sensor	(degrees)
Sensor Azimuth Angle, Cell to Sensor	(degrees)
Brightness Temperature, IR Bands	(K)
Cloud Mask, First Byte	(no units)
Surface Temperature	(K)

Surface Pressure	(hPa)
Processing Flag	(no units)
Tropopause Height	(hPa)
Guess Temperature Profile	(K)
Guess Dew Point Temperature Profile	(K)
Retrieved Temperature Profile	(K)
Retrieved Dew Point Temperature Profile	(K)
Total Ozone Burden	(Dobsons)
Total Totals Index	(K)
Lifted Index	(K)
K Index	(K)
Total Column Precipitable Water Vapor, IR	(cm)
Precipitable Water Vapor Low, IR	(cm)
Precipitable Water Vapor High, IR	(cm)

Retrieval Profile Pressure Levels (hPa)

5, 10, 20, 30, 50, 70, 100, 150, 200, 250, 300, 400, 500, 620, 700, 780, 850, 920, 950, 1000

### **7.0 Future work**

Future work to improve the algorithm will include enhancing the training profile database with more radiosonde observations, particularly in polar areas that are under-represented. Surface emissivity from a global ecosystem database will be used in the training profiles to improve both the regression and physical retrievals. Improvements to the radiance bias corrections are also planned, including adding a seasonal variation to the global radiance values. The relatively high level of noise due to non-uniform detector-to-detector response (striping) will be investigated for possible reduction. Future comparisons with MODIS products will include other ARM-CART sites in the tropical western Pacific and in Barrow, Alaska.

Terra MODIS algorithms have been adapted to the second MODIS instrument that was launched on the Aqua platform on May 4, 2002. The new platform will double the frequency of global coverage and allow for more consistent monitoring of temperature, moisture, and ozone.

In addition, retrievals based on a combination of MODIS and AIRS radiances from Aqua will be investigated to take advantage of the high spectral resolution of AIRS and the high spatial resolution of MODIS.

In the absence of any spectral bands sensitive to the stratosphere (bands with center wavelengths from 14.5 to 15.0  $\mu\text{m}$ ), future profile retrievals from the MODIS may rely on the global numerical forecast models (such as the NCEP Global Data Assimilation System, GDAS) for this information. Since the stratosphere is largely stable and slowly varying, the model should be very representative of the stratospheric conditions and the accuracy of the MODIS temperature and moisture profiles should not be significantly affected.

Improvements to the accuracy of the temperature and moisture profiles are possible with a proper accounting for the surface infrared emissivity characteristics. Plokhenko and Menzel (1999) have shown that it is possible to retrieve shortwave and longwave emissivities along with temperature and moisture profiles in a physical solution using a hemispherical directional effective emissivity model. In surface and profile retrieval calculations with MODIS Airborne Simulator data, their infrared surface emissivity solutions are strongly correlated with vegetation indices inferred from visible data. In addition the atmospheric variations of temperature and moisture were smoother and more physical (Figure 13a). While total column distributions of moisture were not significantly affected, low level mixing ratios (below 850 hPa) were sometimes adjusted by as much as 1 g/kg (Figure 13b). The MODIS Atmospheric Profiles ATBD will be updated to indicate subsequent progress in this work.

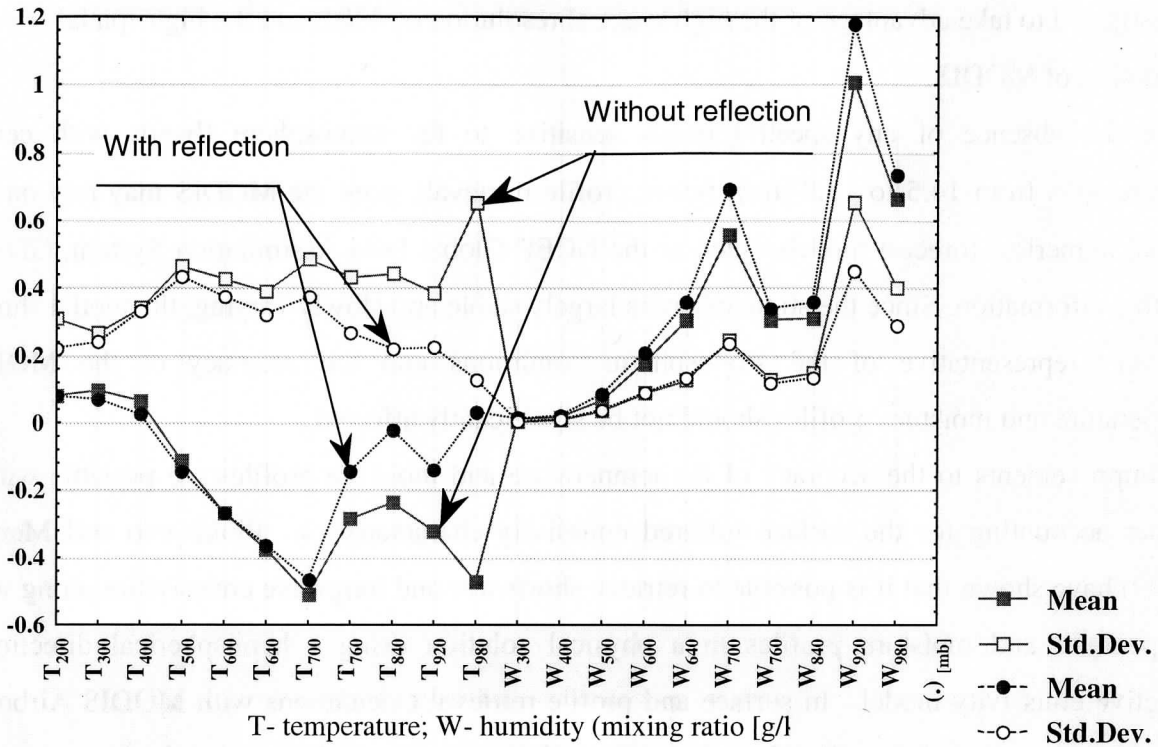


**Figure 13a:** Temperature and mixing ratio profile statistics (mean and standard deviation of first guess adjustment, retrieval minus guess) for the two models (with and without surface reflection).

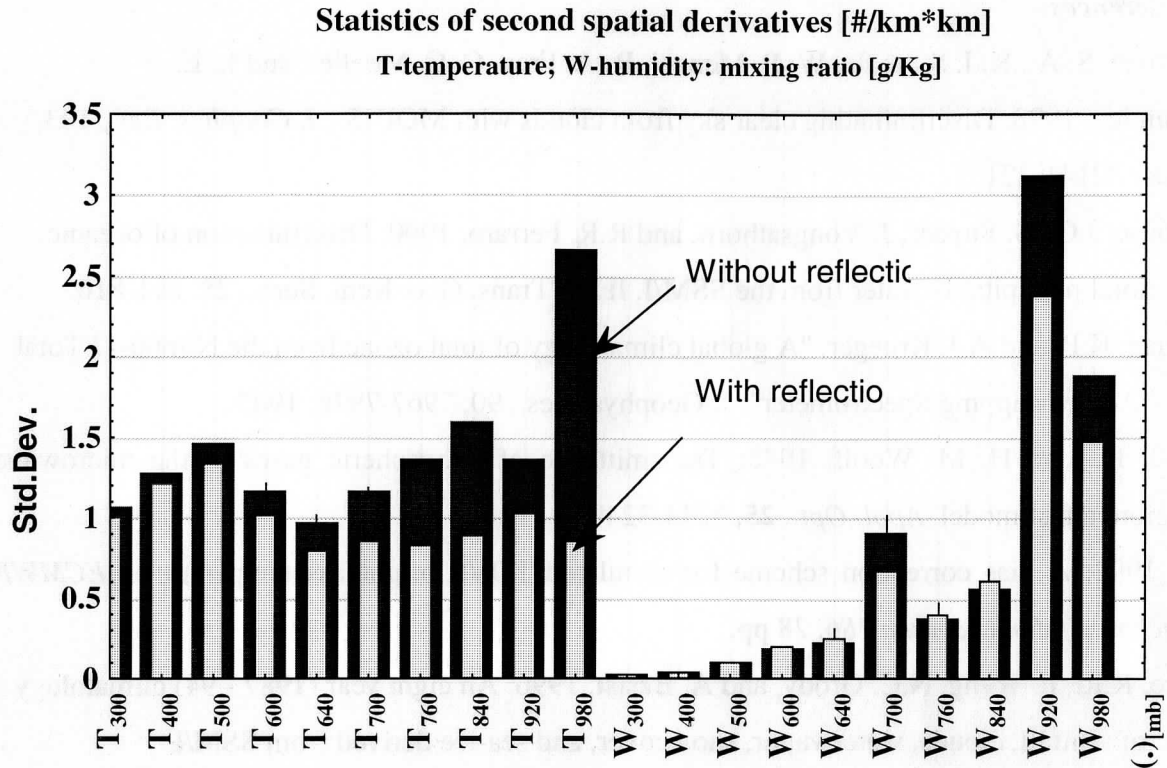


**Figure 13b:** Stability of the solution for the two algorithms (with and without surface reflection) as measured by the standard deviation of the second derivative of the horizontal variation of temperature or mixing ratio at a given level of the atmosphere. Smaller values are more stable and hence better depicting the actual atmospheric state.

## 8. References

- Ackerman, S. A., K. I. Strabala, W. P. Menzel, R. A. Frey, C. C. Moeller, and L. E. Gumley, 1998: Discriminating clear sky from clouds with MODIS. *J. Geophys. Res.*, 103, D24, 32141-32157.
- Alishouse, J.C., S. Snyder, J. Vongsathorn, and R.R. Ferraro, 1990: Determination of oceanic total precipitable water from the SSM/I. *IEEE Trans. Geo. Rem. Sens.*, 28, 811-816.
- Bowman, K.P. and A.J. Krueger, "A global climatology of total ozone from the Nimbus-7 Total Ozone Mapping Spectrometer", *J. Geophys. Res.*, 90, 7967-7976, 1985.
- Eyre, J. R., and H. M. Woolf, 1988: Transmittance of atmospheric gases in the microwave region: a fast model. *Appl. Opt.*, 25, 3244-3249.
- \_\_\_\_\_, 1992: A bias correction scheme for simulated TOVS brightness temperatures. *ECMWF Technical Memorandum 186*. 28 pp.
- Ferraro, R.R., F. Weng, N.C. Grody, and A. Basist, 1996: An eight year (1987 - 94) climatology of rainfall, clouds, water vapor, snowcover, and sea-ice derived from SSM/I measurements. *Bull. of Amer. Meteor. Soc.*, 77, 891 - 905.
- Fleming, H. E. and W. L. Smith, 1971: Inversion techniques for remote sensing of atmospheric temperature profiles. *Reprint from Fifth Symposium on Temperature*. Instrument Society of America, 400 Stanwix Street, Pittsburgh, Pennsylvania, 2239-2250.
- Fritz, S., D. Q. Wark, H. E. Fleming, W. L. Smith, H. Jacobowitz, D. T. Hilleary, and J. C. Alishouse, 1972: Temperature sounding from satellites. *NOAA Technical Report NESS 59*. U.S. Department of Commerce, National Oceanic and Atmospheric Administration, National Environmental Satellite Service, Washington, D.C., 49 pp.
- Hannon, S., L. L. Strow, and W. W. McMillan, 1996: Atmospheric Infrared Fast Transmittance Models: A Comparison of Two Approaches. *Proceeding of SPIE conference 2830, Optical Spectroscopic Techniques and Instrumentation for Atmospheric and Space Research II*.
- Harris, B. A., and G. Kelly, 2001: A satellite radiance bias correction scheme for radiance assimilation. *Quart. J. Roy. Meteor. Soc.*, 127, 1453-1468.
- Hayden, C. M., 1988: GOES-VAS simultaneous temperature-moisture retrieval algorithm. *J. Appl. Meteor.*, 27, 705-733.

- Houghton, J. T., Taylor, F. W., and C. D. Rodgers, 1984: Remote Sounding of Atmospheres. Cambridge University Press, Cambridge UK, 343 pp.
- Kaplan, L. D., 1959: Inference of atmospheric structure from remote radiation measurements. *Journal of the Optical Society of America*, **49**, 1004.
- King, J. I. F., 1956: The radiative heat transfer of planet earth. *Scientific Use of Earth Satellites*, University of Michigan Press, Ann Arbor, Michigan, 133-136.
- King, M.D., Kaufman, Y. J., Menzel, W. P. and D. Tanré, 1992: Remote sensing of cloud, aerosol, and water vapor properties from the Moderate Resolution Imaging Spectrometer
- Li, J., and H.-L. Huang, 1999: Retrieval of atmospheric profiles from satellite sounder measurements by use of the discrepancy principle, *Appl. Optics*, Vol. 38, No. 6, 916-923.
- Li, J., W. Wolf, W. P. Menzel, W. Zhang, H.-L. Huang, and T. H. Achtor, 2000: Global soundings of the atmosphere from ATOVS measurements: The algorithm and validation, *J. Appl. Meteorol.*, **39**: 1248 – 1268.
- Ma, X. L., Schmit, T. J. and W. L. Smith, 1999: A non-linear physical retrieval algorithm – its application to the GOES-8/9 sounder. Accepted by *J. Appl. Meteor.*
- McPeters, R.D, Krueger, A.J., Bhartia, P.K., Herman, J.R. et al, 1996, "Nimbus-7 Total Ozone Mapping Spectrometer (TOMS) Data Products User's Guide", NASA Reference Publication 1384, available from NASA Center for Aerospace Information, 800 Elkridge Landing Rd, Linthicum Heights, MD 21090, USA; (301) 621-0390.
- McPeters, R.D, Krueger, A.J., Bhartia, P.K., Herman, J.R. et al, 1998, "Earth Probe Total Ozone Mapping Spectrometer (TOMS) Data Products User's Guide", NASA Reference Publication 1998-206895, available from NASA Center for Aerospace Information, 800 Elkridge Landing Rd, Linthicum Heights, MD 21090, USA; (301) 621-0390.
- Menzel, W. P., and J. F. W. Purdom, 1994: Introducing GOES-I: The first of a new generation of geostationary operational environmental satellites. *Bull. Amer. Meteor. Soc.*, **75**, 757-781.
- Menzel, W. P., F. C. Holt, T. J. Schmit, R. M. Aune, A. J. Schreiner, G. S. Wade, and D. G. Gray, 1998. Application of the GOES-8/9 soundings to weather forecasting and nowcasting. *Bull. Amer. Meteor. Soc.*, **79**, 2059-2077.



- Plokhenko, Y. and W. P. Menzel, 1999: The effects of surface reflection on estimating the vertical temperature – humidity distribution from spectral infrared measurements. Submitted to *J. Appl. Meteor*
- Rodgers, C. D., 1976: Retrieval of atmospheric temperature and composition from remote measurements of thermal radiation. *Rev. Geophys. Space Phys.*, **14**, 609-624.
- Salisbury, J.W., and D.M. D’Aria, 1992: Emissivity of terrestrial materials in the 8-14mm atmospheric window. *Remote Sensing of the Environment*, **42**, 83-106.
- Schmit, T. J., Feltz, W. F., Menzel, W. P., Jung, J., Noel, A. P., Heil, J. N., Nelson, J. P., and G.S.Wade, 2002: Validation and Use of GOES Sounder Moisture Information. *Wea. Forecasting*, **17**, 139-154.
- Smith, W. L., Woolf, H. M., and W. J. Jacob, 1970: A regression method for obtaining real-time temperature and geopotential height profiles from satellite spectrometer measurements and its application to Nimbus 3 “SIRS” observations. *Mon. Wea. Rev.*, **8**, 582-603.
- \_\_\_\_\_, Woolf, H. M., Hayden, C. M., Wark, D. Q. and L. M. McMillin, 1979: The TIROS-N operational vertical sounder. *Bull. Amer. Meteor. Soc.*, **60**, 1177-1187.
- \_\_\_\_\_, Suomi, V. E., Menzel, W. P., Woolf, H. M., Sromovsky, L. A., Revercomb, H. E., Hayden, C. M., Erickson, D. N. and F. R. Mosher, 1981: First sounding results from VAS-D. *Bull. Amer. Meteor. Soc.*, **62**, 232-236.
- \_\_\_\_\_, and F. X. Zhou, 1982: Rapid extraction of layer relative humidity, geopotential thickness, and atmospheric stability from satellite sounding radiometer data. *Appl. Opt.*, **21**, 924-928.
- \_\_\_\_\_, and H. M. Woolf, 1988: A Linear Simultaneous Solution for Temperature and Absorbing Constituent Profiles from Radiance Spectra. Technical Proceedings of the Fourth International TOVS Study Conference held in Igls, Austria 16 to 22 March 1988, W. P. Menzel Ed., 330-347.
- \_\_\_\_\_, 1991: Atmospheric soundings from satellites - false expectation or the key to improved weather prediction. *Jour. Roy. Meteor. Soc.*, **117**, 267-297.
- \_\_\_\_\_, Woolf, H. M., Nieman, S. J., and T. H. Achtor, 1993: ITPP-5 - The use of AVHRR and TIGR in TOVS Data Processing. Technical Proceedings of the Seventh International TOVS Study Conference held in Igls, Austria 10 to 16 February 1993, J. R. Eyre Ed., 443-453.



Twomey, S., 1977: An introduction to the mathematics of inversion in remote sensing and indirect measurements. Elsevier, New York.

Wark, D. Q., 1961: On indirect temperature soundings of the stratosphere from satellites. *J. Geophys. Res.*, **66**, 77.

\_\_\_\_\_, Hilleary, D.T., Anderson, S. P., and J. C. Fisher, 1970: Nimbus satellite infrared spectrometer experiments. *IEEE. Trans. Geosci. Electron.*, **GE-8**, 264-270.

Wentz F. J. 1997, "A well-calibrated ocean algorithm for SSM/I", *J. Geophys. Res.*, Vol. 102, No. C4, pg. 8703-8718.